Materials and Design 51 (2013) 331–341

Contents lists available at SciVerse ScienceDirect

Materials and Design

journal homepage: www.elsevier.com/locate/matdes

Influence of reinforcements (SiC and Al_2O_3) and rotational speed on wear and mechanical properties of aluminum alloy 6061-T6 based surface hybrid composites produced via friction stir processing

A. Devaraju [a], A. Kumar [a,*], A. Kumaraswamy [b], B. Kotiveerachari [a]

[a] Department of Mechanical Engineering, National Institute of Technology, Warangal, AP, India
[b] Department of Mechanical Engineering, Defense Institute of Advanced Technology, Pune, Maharashtra, India

ARTICLE INFO

Article history:
Received 14 October 2012
Accepted 9 April 2013
Available online 20 April 2013

Keywords:
Friction stir processing
Surface hybrid composites
Wear
Microstructure
Mechanical properties
Analysis of variance

ABSTRACT

In this investigation, the influence of rotational speed and reinforcement particles such as silicon carbide (SiC), alumina (Al_2O_3) on wear and mechanical properties of aluminum alloy based surface hybrid composites fabricated via friction stir processing (FSP) was studied. Taguchi method was employed to optimize the rotational speed and volume percentage of reinforcement particles for improving the wear and mechanical properties of surface hybrid composites. The fabricated surface hybrid composites have been examined by optical microscope for dispersion of reinforcement particles. Microstructures of all the surface hybrid composites revealed that the reinforcement particles (SiC and Al_2O_3) are uniformly dispersed in the nugget zone. It also revealed that the microhardness at optimum condition is increased due to presence and pining effect of hard SiC and Al_2O_3 particles. It is found that the reinforcement particles (i.e. SiC and Al_2O_3) reduced in size (~5 μm) than the as received particles size and also observed that the wear resistance at optimum condition is immensely improved. The observed wear and mechanical properties have been correlated with microstructures and worn micrographs.

1. Introduction

Aluminum alloy 6061-T6 is widely utilized in aircraft, defense, automobiles and marine areas due to their good strength, light weight and better corrosion properties. But, they exhibits inferior tribological properties in extensive usage [1,2]. In addition, aluminum based composites become brittle by the addition of reinforcements such as SiC and Al_2O_3 ceramic particles [3].

A proper technique can be employed to refine the microstructure and homogeneous dispersion of reinforcements on metallic surface as since wear is a surface deprivation property [4]. Dispersion of reinforcement particles on metal surface and the control of its dispersal are more difficult to attain by conventional surface modification techniques [5]. Guptha et al. [6] and Mabhali et al. [7] reported that the thermal spraying and laser beam techniques were utilized to prepare surface composites, in which it degrades the properties due to formation of unfavourable phases. These techniques are operated at higher temperatures and impossible to avoid the reaction between the reinforcements and the matrix, which forms a detrimental phase. Therefore a process can be employed which is operated at below melting temperature of matrix for the fabrication of surface composites which can be used to avoid the above mentioned complications.

Considering the above problems, FSP is best suited for preparation of surface composites and surface modification. In FSP a rotating tool with shoulder and pin is plunged into the surface of material, which creates frictional heat and dynamic mixing of material area underneath the tool [8], it leads to incorporation and/or dispersion of the reinforcement particles in the matrix material such as aluminum alloys, Magnesium alloys and Copper [9–11]. Devaraju et al. [12] achieved homogeneous dispersion of SiC particles (20 μm average size) on a surface of aluminum alloy 6061-T6 via FSP. Hybrid composites are prepared by reinforcing with a mixture of two or more different type of particles which combines the individual properties of each type of particle. Essam et al. [13] fabricated Al-1050-H24/(20%Al_2O_3 + 80%SiC) hybrid composite via FSP and exhibited high hardness and superior wear resistance than the matrix material.

However, it has not been found and yet no result was reported for improvement of wear and mechanical properties by the addition of mixture of SiC and Al_2O_3 particles as refinements on the surface of aluminum alloy 6061-T6 via FSP. The optimization of rotational speed and volume percentage of reinforcements for improving the wear properties of aluminum alloy 6061-T6/(SiC + Al_2O_3) surface hybrid composites was not reported. Taguchi

* Corresponding author. Tel.: +91 9492783067; fax: +91 08702462834.
E-mail addresses: aruri_devaraj@yahoo.com (A. Devaraju), adepu_kumar7@yahoo.co.in, adepu_kumar7@nitw.ac.in (A. Kumar), akswamy@diat.ac.in (A. Kumaraswamy), bkvachari@hotmail.com (B. Kotiveerachari).

0261-3069/$ - see front matter © 2013 Elsevier Ltd. All rights reserved.
http://dx.doi.org/10.1016/j.matdes.2013.04.029

Table 1
Chemical composition of aluminum 6061-T6 alloy (Wt.%).

Element	Mg	Si	Cu	Zn	Ti	Mn	Cr	Al
Amount (wt.%)	0.85	0.68	0.22	0.07	0.05	0.32	0.06	Balance

method is a systematic methodology intended for design and analysis of experiments to improve the quality characteristics [14–16]. Nowadays, it has become a very popular practical tool for improving the quality of output without increasing the cost of experimentation by reducing the number of experiments. Mallaiah et al. [17] optimized mechanical properties of TIG welded Ferritic Stainless steels by using Taguchi method. The objective of present investigation is to study the influence of reinforcement particles and rotational speed on wear and mechanical properties of aluminum alloy 6061-T6/(SiC + Al_2O_3) surface hybrid composites fabricated via FSP and to obtain the optimum combinations using Taguchi method.

2. Experimental procedure

The base material employed in this study is 4 mm thick aluminum alloy 6061-T6. The chemical composition of the base material is given in Table 1.

The reinforcement particles which have effect on the wear and mechanical properties were identified as SiC and Al_2O_3 [13,18–21]. The Scanning electron microscope (SEM) micrographs of as received SiC and Al_2O_3 particles are shown in Fig. 1.The average size of both reinforcement particles are 20 μm.

The square groove was made with dimensions of 3 mm width and 3 mm depth tangent to the pin in the advancing side and which is 1 mm far away from the centre line of the tool rotation on the aluminum alloy 6061-T6 plate. The schematic sketch of aluminum alloy plate for FSP is shown in Fig. 2. H13 tool steel having screwed taper pin profile with shoulder diameter of 24 mm, pin diameter of 8 mm and 3.5 mm height was used.

The reinforcement mixtures of SiC and Al_2O_3 particles at selected ratios were packed in the groove. The groove opening was initially closed by means of the tool which is having shoulder without pin to avoid the escapement of reinforcement particles from groove while processing. The tool traveling speed of 40 mm/min, axial force of 5 KN and tool onward tilt angle of 2.5° along the centre line were used in FSP. The experiments are carried out on a Vertical milling machine (Make HMT FM-2, 10 hp, 3000 rpm). All the experiments are to be carried out with constant axial force and constant traverse speed. Finally, the temperature is controlling mechanism to obtain fine grain structure. This final temperature is mainly depends on the axial force, rotational speed, tool pin profile, shoulder diameter and traverse speed etc.. The authors are optimized the welding speed, shoulder diameter, and pin profile in previous research work on the same material i.e. 6061-T6 aluminum alloy.

For various testing, samples were cut with required dimensions as per ASTM standards from the FSP nugget zone by using wire-cut Electrical discharge machining (EDM). The schematic diagram of selection of samples for testing is shown in Fig. 3.

After FSP, microstructural observations were carried out at the cross section of nugget zone (NZ) of surface hybrid composites normal to the FSP direction, mechanically polished and etched with Keller's reagent (2 ml HF, 3 ml HCl, 20 ml HNO_3 and 175 ml H_2O) by employing optical microscope (OM). The SEM is also utilized for measuring the reinforcement particles size and worn morphology of surface hybrid composites.

Microhardness tests were carried out at the cross section of NZ of surface hybrid composites normal to the FSP direction, samples were tested with a load of 15 g and duration of 15 sec using a Vickers digital microhardness tester.

The tensile specimens were taken from the surface hybrid composites normal to the FSP direction and made as per ASTM: E8/E8M-11 standard by using Wire cut Electrical Discharge Machining to the required dimensions. The schematic sketch of tensile specimen is shown in Fig. 4. The tensile test is carried out on a computer controlled universal testing machine at a cross head speed of 0.5 mm/min.

Wear test is carried out on a pin-on-disk tribometer as per ASTM: G99-05 standard. Prismatic pins of 8 mm diameter were cut from the NZ, with the axis of the pin normal to the FSP direction. The disk was made of EN31 steel with hardness of 62 HRC. The diameter of the sliding track on the disk surface was 100 mm. The wear tests were performed under dry sliding conditions with a constant load (40 N), rotational speed (650 rpm) and sliding speed (3.4 m/s). The schematic configuration of pin-on-disk is shown in Fig. 5.

Wear rate is calculated by,

$$\text{Wear rate } (\text{mm}^3/\text{m}) = \text{Volume loss}/\text{Sliding distance}$$

2.1. Planning of experiments based on Taguchi's method

Rotational speed is the most important process parameter in FSP which has greater influence in uniform distribution of reinforcement particles, grain refinement and heat input during the process [8,22,23]. Trial experiments were conducted by varying the volume percentage of the reinforcement particles and keeping the other parameters constant to find the working range of volume

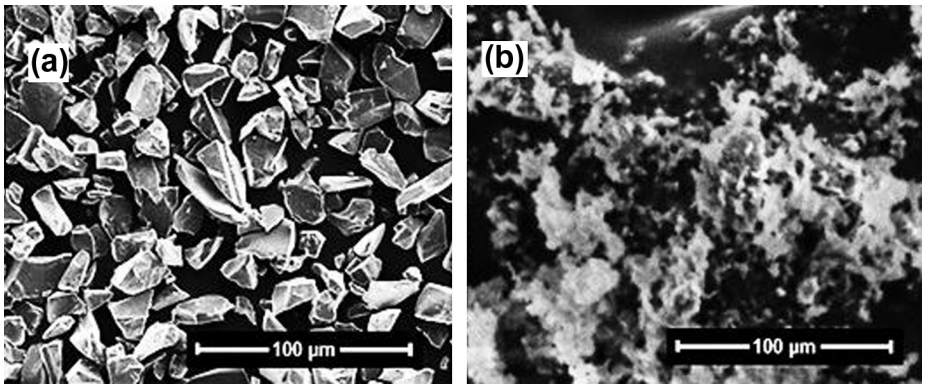

Fig. 1. SEM micrographs of as-received (a) SiC and (b) Al_2O_3 particles.

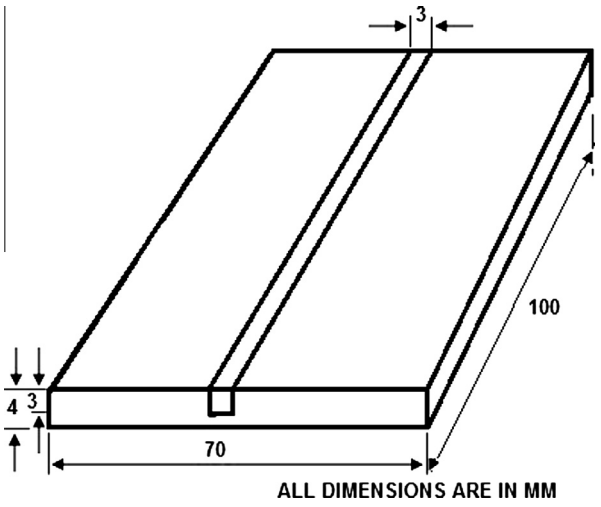

Fig. 2. Schematic sketch of aluminum alloy plate for FSP.

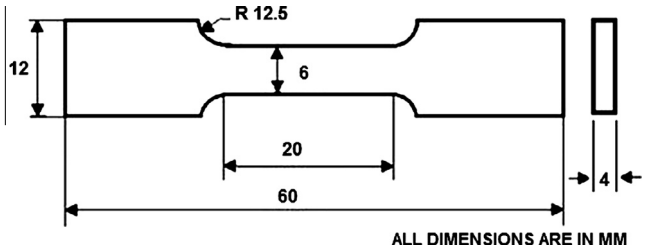

Fig. 4. Schematic sketch of tensile specimen.

percentage of reinforcement particles in such that the surface hybrid composites should be free from defects. The working range of selected parameters and the constant process parameters were presented in Table 2 and 3 respectively.

Taguchi's method is very effective to deal with responses influenced by many parameters. It is a simple, efficient and systematic approach to determine optimal process parameters. It is a powerful design of experiments tool which reduces drastically the number of experiments that are required to model and optimize the responses. Also, it saves lot of time and experimental cost [14–16]. The Taguchi method is devised for process optimization and identification of optimum levels of process parameters for given responses. In Taguchi method, the experimental values of various responses are further transformed to signal to noise (S/N) ratio. The response that is to be maximized is called 'Higher the better' and the response that is to be minimized is called 'Lower the better'. Taguchi uses the S/N ratio to measure deviation of the response from the mean value. S/N ratios for 'Higher the better' and 'Lower the better' characteristics are calculated using Eqs. (1) and (2) respectively,

$$\eta = -10\log_{10}\left[\frac{1}{n}\sum_{i=1}^{n}\frac{1}{y_i^2}\right] \quad (1)$$

$$\eta = -10\log_{10}\left[\frac{1}{n}\sum_{i=1}^{n}y_i^2\right] \quad (2)$$

where η denotes S/N ratio of experimental values, y_i represents the experimental value of the ith experiment and n is the total number of experiments.

In the present study, the Taguchi method was applied to experimental data using statistical software MINITAB-15. The number of process parameters considered under this study is three and the level of each factor is three. The degree of freedom of all the three factors is 6. Hence, L_9 (3^4) orthogonal array is selected. Each condition of experiment was repeated twice in order to reduce the noise/error effects. The selected orthogonal array is presented in Table 4.

The quality characteristics such as wear rate (WR), ultimate tensile strength (UTS), yield strength (YS), percentage of elongation (%EL) and microhardness of surface hybrid composites were evaluated for all the trials and then statistical analysis of variance (ANOVA) was carried out. Based on the ANOVA, the contribution of each element in influencing the quality characteristic is evaluated. The optimum element combinations were predicted and verified.

3. Results and discussions

3.1. Microstructure

The optical micrographs of all the surface hybrid composites (Exp. 1–9) are shown in Fig. 6. The particles of SiC and Al_2O_3 were observed to be dispersed uniformly in the NZ for all the conditions of composites made by FSP as the rotating tool gives sufficient heat generation and a circumferential force to distribute the reinforcement particles to flow in a wider area [12,13]. The SEM micrographs of SiC and Al_2O_3 particles after FSP are shown in Fig. 7 and 8 respectively.

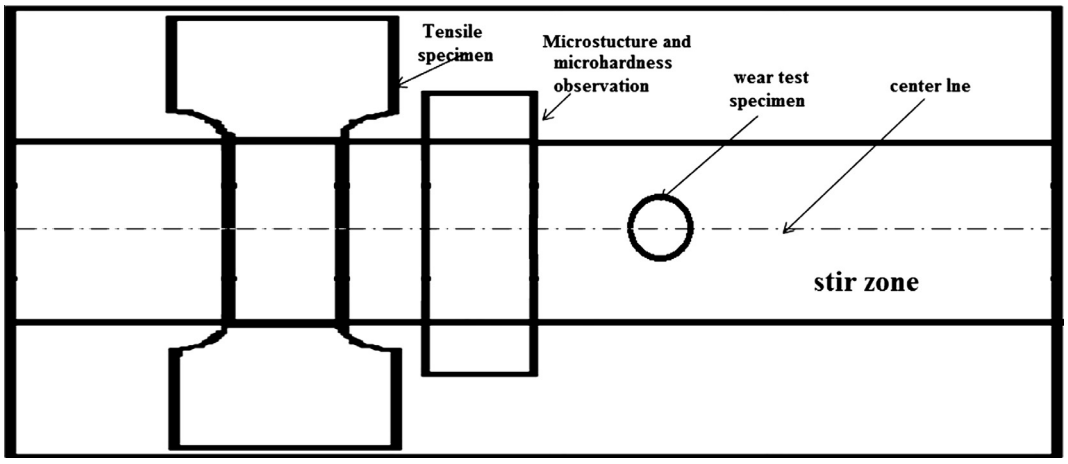

Fig. 3. Schematic diagram of selection of sample for testing.

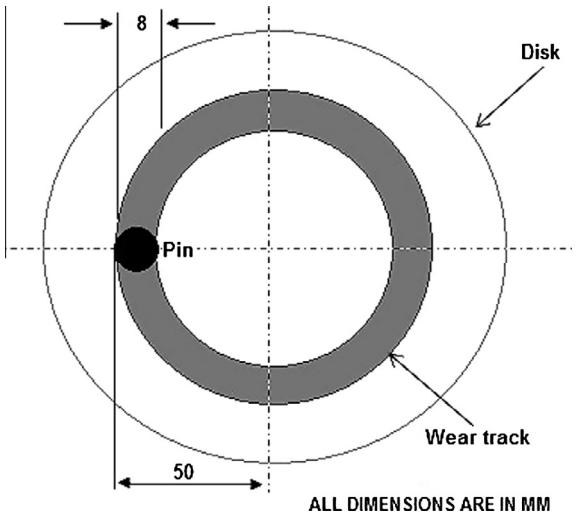

Fig. 5. Schematic configuration of pin-on-disc tribo meter.

Table 2
Working range of the selected parameters.

Symbol	Parameters	Units	Level		
			(1)	(2)	(3)
A	Rotational speed	rpm	900	1120	1400
B	SiC_p	vol.%	8	6	4
C	Al_2O_{3p}	vol.%	2	3	4

Table 3
Constant process parameters.

Parameters	Value
Tool traverse speed	40 mm/min
Tool vertical force	5 KN
Tool tilt angle	2.5°
Tool pin profile	Taper with threaded
Tool shoulder diameter	24 mm
Tool pin diameter	8 mm
D_s/D_p ratio	3
Number of passes	1

Table 4
Experimental layout L_9 (3^4) orthogonal array.

Exp. no.	A	B	C
1	1	1	1
2	2	2	2
3	3	3	3
4	1	2	3
5	2	3	1
6	3	1	2
7	1	3	2
8	2	1	3
9	3	2	1

It is found that the size of the reinforcement particles (i.e. SiC and Al_2O_3) were reduced in size (~5 μm) than the as received particles and it is due to the tool which provides a shear force to substantial breaking of reinforcement particles in NZ and intense plastic deformation [8]. It is also observed that the micro void is formed around the Al_2O_3 particle not for SiC particles which is due to the Al_2O_3 particles having poor wettability with Al matrix [13].

3.2. Mechanical and wear properties

The microhardness, UTS, YS, %EL and wear rate of surface hybrid composites and base metal were evaluated and presented in Table 5. Regression analysis is used to evaluate the data on all the properties of surface hybrid composite. These developed regression equations are used in predicting the microhardness, UTS, YS, %El and wear rate within the factorial space exploited.

3.2.1. Development of regression models

The regression model commonly used is represented by $Y = f(A, B \text{ and } C)$. Y denotes the performance characteristics and A, B and C are the process parameters. The general regression model consisting of only linear and quadratic effects is given by the Eq. (3),

$$Y = \beta_0 + \beta_1 A + \beta_2 B + \beta_3 C + \beta_4 A^2 + \beta_5 B^2 + \beta_6 C^2 + \varepsilon \quad (3)$$

where β_0, $\beta_1, \ldots, \beta_6$ are the regression coefficients of process parameters and ε is the experimental error. The developed regression equations and correlation coefficients for the observed properties were summarized in Table 6.

High correlation coefficient indicates good relationship between the process parameters and the observed property data. The coefficient of correlation (R^2) is defined as the ratio of explained variation to the total variation and it's a measure of degree of fit of the model, when it approaches to unity, the developed model fits the actual data with given confidence. All models have higher values of R^2 i.e. above 95%, which means that the regression model provides an excellent explanation of relationship between parameters and responses. All these models are statistically significant at 95% confidence level.

3.2.2. Optimization and validation of process parameters performance characteristics

The optimization of volume percentage of reinforcement particles and rotational speed using Taguchi method permits evaluation of the effects of individual elements independent of other elements on the identified quality characteristics, i.e. microhardness, UTS, YS, %EL and wear rate. The influence of each reinforcement particles and rotational speed can be evaluated by determining the S/N ratio for each factor at each level. The S/N ratio response graphs for various responses are shown in Figs. 9–13. From the main effect plots analysis, the optimum parametric combinations for better wear and mechanical properties are obtained and summarized in Table 7.

The predicted values for various responses at optimum condition are calculated using the predicted S/N ratio (η_{opt}) Eq. (4),

$$\eta_{opt} = \eta_m + \sum_{i=1}^{j} (\eta_{jm} - \eta_m) \quad (4)$$

where η_{jm} is the mean S/N ratio of optimum level and j is the number of process parameters that affect the response. For validation of the optimum results, experiments are conducted at optimum condition and the results are presented in Table 8. It is observed that experimental values were closer to the optimum values.

3.2.3. Analysis of variance (ANOVA)

In order to find the effect of process parameters on various responses, ANOVA is performed and the results are presented in Table 9. The calculated F-values of the ANOVA for various responses determine the relative significances of different process parameters. Results of ANOVA revealed that the reinforcement particles (SiC and Al_2O_3) and rotational speed have significant effect on all the quality characteristics. It is clear from the ANOVA Table 9 that, the rotational speed has less percentage of contribution on the wear rate compared to SiC and Al_2O_3 volume percentage.

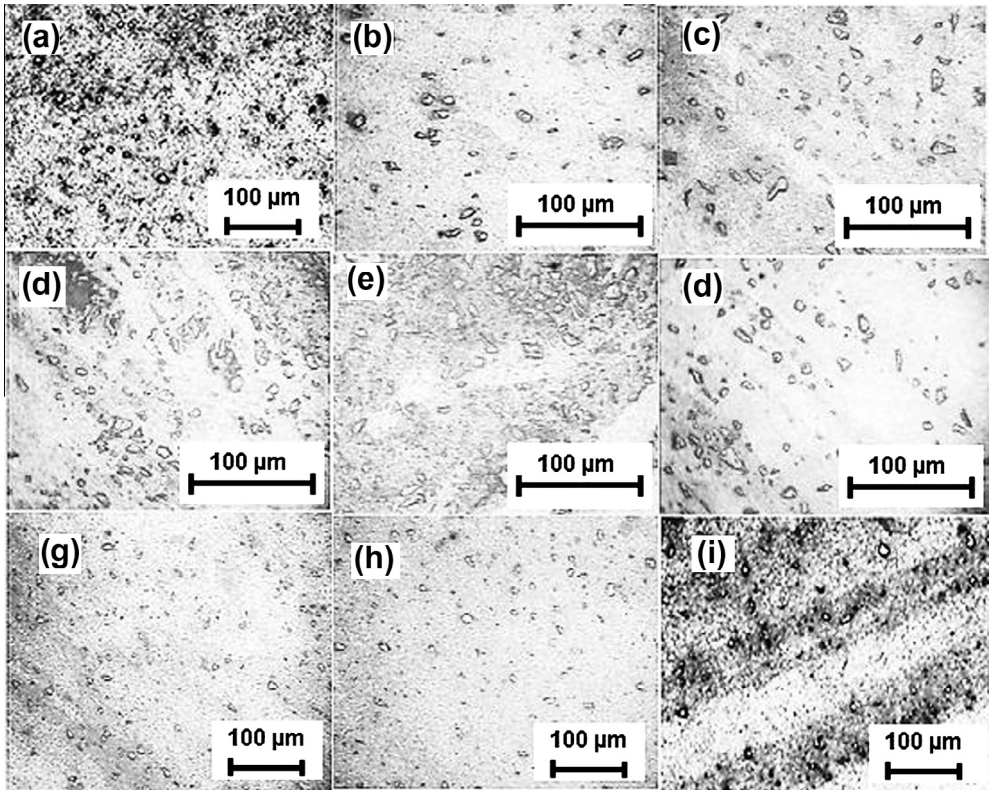

Fig. 6. Optical microstructures of all the surface hybrid composites (a) Exp. 1, (b) Exp. 2, (c) Exp. 3, (d) Exp. 4, (e) Exp. 5, (f) Exp. 6, (g) Exp. 7, (h) Exp. 8 and (i) Exp. 9.

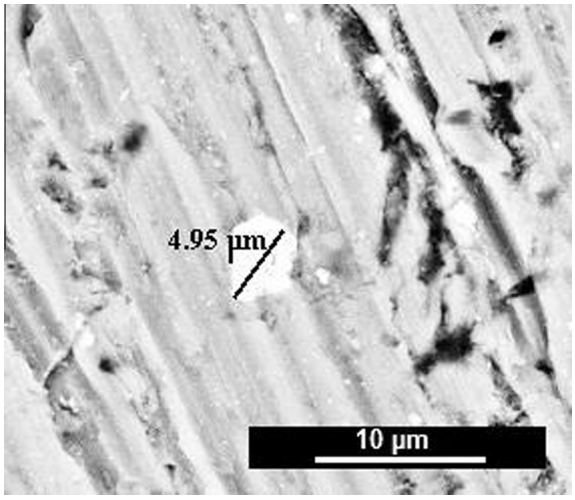

Fig. 7. SEM micrograph of SiC reinforcement particle after FSP.

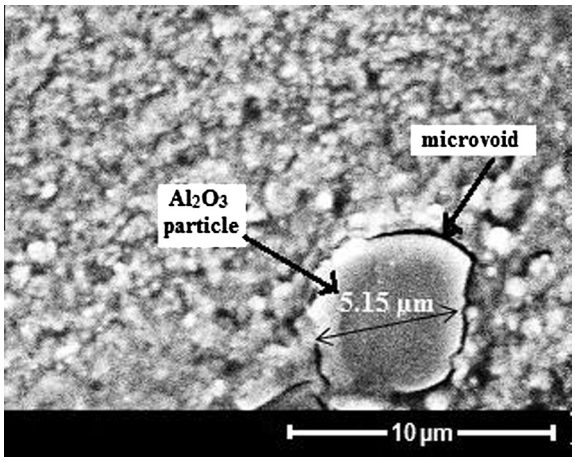

Fig. 8. SEM micrograph of Al_2O_3 reinforcement particle after FSP.

3.2.4. Effect of process parameters on microhardness

The S/N ratio response graph for microhardness is shown in Fig. 9. It is revealed that as the rotational speed increases the microhardness also increases which is due to the increase in heat input that causes easier and more intense stirring action of the rotating pin resulting in better dispersion of reinforcement particles thus increasing the microhardness. Further increasing the rotational speed decreases the microhardness. This is due to the high heat generation that causes matrix softening which decreases the microhardness. This softening of the NZ is resulted in coarsening and/or dissolution of strengthening precipitates in the aluminum matrix which occurs especially in heat treatable aluminum alloys [24].

It is observed that the increase in the volume percentage of SiC and Al_2O_3 particles immensely increases the microhardness due to the presence and pinning effect of the SiC and Al_2O_3 particles [8,9,12,13]. The presence of SiC particles is considered for more effective formation of fine grain structure due to the restrain of grain boundary and the enhancement of the induced strain [25]. However the higher hardness is achieved by the SiC and Al_2O_3 particles.

Mainly, the microhardness value depends on the presence and uniform distribution of SiC and Al_2O_3 particles. The optimum microhardness value was obtained at the optimum condition of 1120 rpm, 8 volume percentage of SiC and 4 volume percentage of Al_2O_3. This is due to fact that at 1120 rpm, tool shoulder supplied

Table 5
Wear and mechanical properties of aluminum 6061-T6 alloy surface hybrid composites.

Exp. no.	Micro hardness at NZ (Hv)		Ultimate tensile strength (UTS, MPa)		Yield strength (YS, MPa)		Percentage of elongation (%EL)		Wear rate (mm^3/m)	
	Trail 1	Trail 2	Trail 1	Trail 2	Trail 1	Trail 2	Trail 1	Trail 2	Trail 1	Trail 2
1	115	109	132	148	104	120	6.2	7.4	0.002005	0.002031
2	105	115	138	152	111	125	5.8	6.2	0.003173	0.003205
3	111	97	134	142	99	107	5.9	6.7	0.003234	0.003272
4	104	120	152	168	126	142	6.5	7.9	0.002391	0.002415
5	102	118	147	163	114	130	7.3	6.7	0.003404	0.003438
6	124	112	127	141	95	109	6.1	6.5	0.003139	0.003167
7	101	85	183	195	141	153	7.8	8.8	0.003604	0.003642
8	125	139	103	121	74	92	4.9	5.8	0.002587	0.002617
9	110	98	131	147	98	114	5.6	6.8	0.002332	0.002368
Base material	102	106	285	303	263	279	11.5	12.5	0.005274	0.005280

Table 6
Regression equations for the microhardness, UTS, YS, %EL and wear rate of surface hybrid composites.

Sl. no.	Response	Regression equation	Coefficient of correlation R-sq (%)
1.	Micro hardness (Hv)	$Hv = 81.8 + 0.392 * A - 3.92 * B - 28.3 * C - 0.000168 * A^2 + 0.708 * B^2 + 5.33 * C^2$	96.0
2.	UTS (MPa)	$UTS = 405 - 0.583 * A + 2.0 * B + 88.0 * C + 0.000231 * A^2 - 0.83 * B^2 - 15.3 * C^2$	96.7
3.	YS (MPa)	$YS = 291 - 0.477 * A + 17.2 * B + 70.7 * C + 0.000184 * A^2 - 1.96 * B^2 - 12.3 * C^2$	95.7
4.	%EL	$\%EL = 20.7 - 0.0267 * A - 0.367 * B + 3.20 * C + 0.000011 * A^2 + 0.0083 * B^2 - 0.567 * C^2$	97.3
5.	Wear rate (mm^3/m)	$WR = 0.00490 + 0.000011 * A - 0.00130 * B + 0.00396 * C - 0.000000 * A^2 + 0.000091 * B^2 - 0.000647 * C^2$	98.0

Table 7
Optimum values of the quality characteristics.

Quality characteristics	Optimum condition	Optimum value
Microhardness at NZ (Hv)	A2, B1, C3 i.e., rotational speed at 1120 SiC vol.% at 8 Al_2O_3 vol.% at 4	133.97
UTS (MPa)	A1, B3, C2 i.e., rotational speed at 900 SiC vol.% at 4 Al_2O_3 vol.% at 3	190.53
YS (MPa)	A1, B3, C2 i.e., rotational speed at 900 SiC vol.% at 4 Al_2O_3 vol.% at 3	152.07
%EL	A1, B3, C2 i.e., rotational speed at 900 SiC vol.% at 4 Al_2O_3 vol.% at 3	8.46
Wear rate (mm^3/m)	A1, B1, C1 i.e., rotational speed at 900 SiC vol.% at 8 Al_2O_3 vol.% at 2	0.002079

Table 8
Validation of the optimum results.

Quality characteristics	Optimum condition	Optimum value	Experimental value
Microhardness at NZ (Hv)	A2, B1, C3 i.e., rotational speed at 1120 SiC vol.% at 8 Al_2O_3 vol.% at 4	133.97	132
UTS (MPa)	A1, B3, C2 i.e., rotational speed at 900 SiC vol.% at 4 Al_2O_3 vol.% at 3	190.53	189
YS (MPa)	A1, B3, C2 i.e., rotational speed at 900 SiC vol.% at 4 Al_2O_3 vol.% at 3	152.07	147
%EL	A1, B3, C2 i.e., rotational speed at 900 SiC vol.% at 4 Al_2O_3 vol.% at 3	8.46	8.3
Wear rate (mm^3/m)	A1, B1, C1 i.e., rotational speed at 900 SiC vol.% at 8 Al_2O_3 vol.% at 2	0.002079	0.002018

* Average of two values.

Table 9
ANOVA results for various responses.

Process parameter	Degree of freedom (DF)	Sum of squares (SS)	Adj. mean sum of squares (MSS)	*F*-ratio	*P*	% of Contribution
(a) for Microhardness						
A	2	220.22	110.11	6.08	0.141	23.82
B	2	520.22	260.11	14.36	0.065	56.75
C	2	137.56	68.78	3.80	0.208	14.45
Error	2	36.22	18.11			4.98
Total	8	914.22				100
(b) for UTS						
A	2	1334.9	667.44	11.49	0.08	35.51
B	2	1558.2	779.11	13.41	0.069	45.30
C	2	566.2	283.11	4.87	0.17	16.02
Error	2	116.2	58.11			3.17
Total	8	3575.6				100
(c) for YS						
A	2	1307.6	653.78	10.53	0.087	42.01
B	2	1060.2	530.11	8.53	0.105	38.56
C	2	370.9	185.44	2.99	0.251	14.06
Error	2	124.2	62.11			5.37
Total	8	2862.9				100
(d) for %EL						
A	2	2.7222	1.36111	18.28	0.052	48.14
B	2	1.7089	0.85444	11.48	0.08	31.42
C	2	0.8822	0.44111	5.93	0.144	16.70
Error	2	0.1489	0.07444			3.74
Total	8	5.4622				100
(e) for Wear rate						
A	2	0.000000	0.00000	4.70	0.175	12.21
B	2	0.000001	0.000001	27.01	0.036	49.55
C	2	0.000001	0.000000	17.79	0.053	35.73
Error	2	0.000000	0.000000			2.51
Total	8	0.000002				100

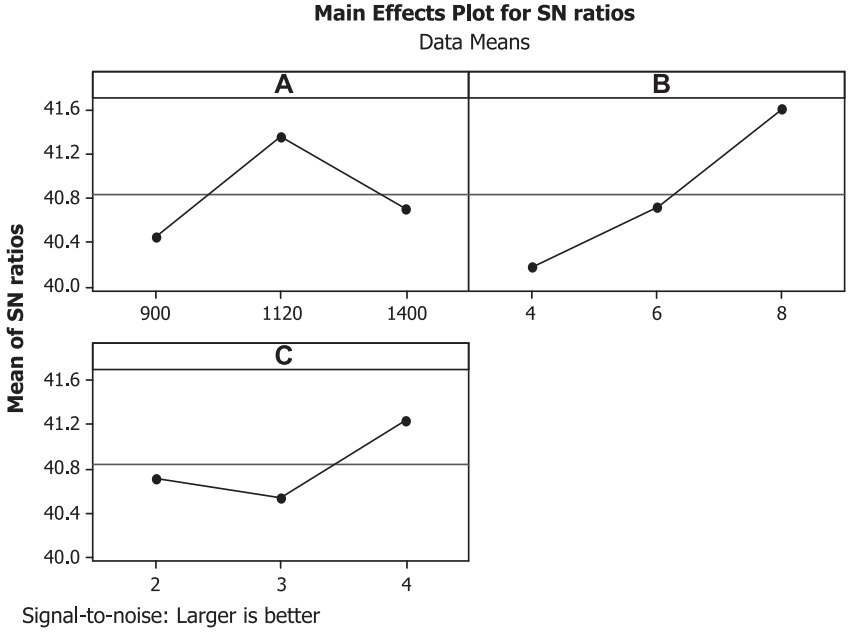

Fig. 9. S/N ratio response graph for microhardness.

enough heat input and shear force to make the reinforcement particles more easily wrapped by the softened metal and rotated with FSP tool which results in well separation and distribution in the nugget zone.

3.2.5. Effect of process parameters on tensile properties

The S/N ratio response graphs for UTS, YS and %EL are shown in Fig. 10–12 respectively. It is revealed that as the rotational speed increases the UTS, YS and %EL decreases and however as earlier mentioned, the heat input increases with increase of rotational speed [22] which resulted in matrix softening. Actually the softening of material will improve the %EL but contrary in this; the %EL decreases a very less as rotational speed increases due to loss in strength of the matrix.

It is observed that the increase in the volume percentage of SiC particles, the UTS, YS and %EL immensely decreases. However,

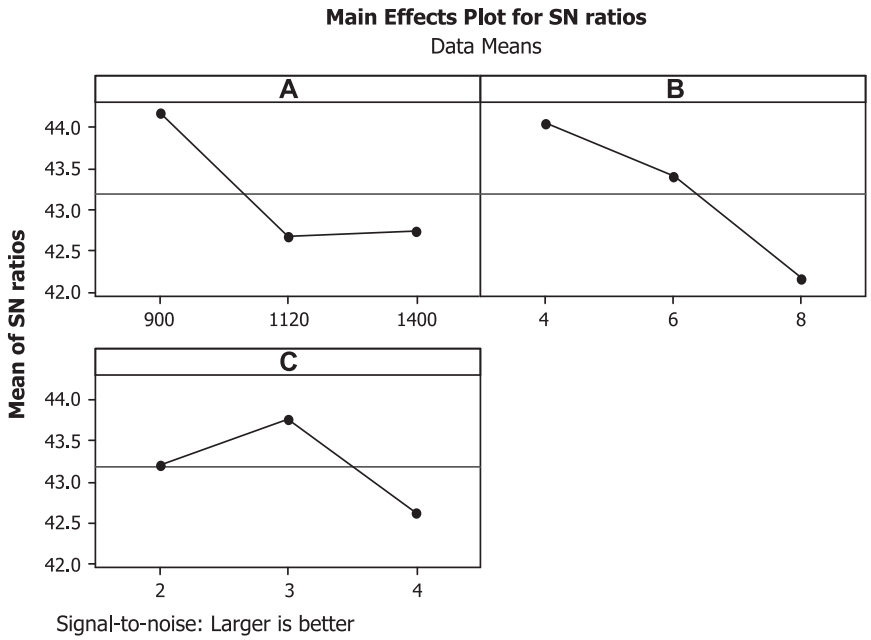

Fig. 10. S/N ratio response graph for UTS.

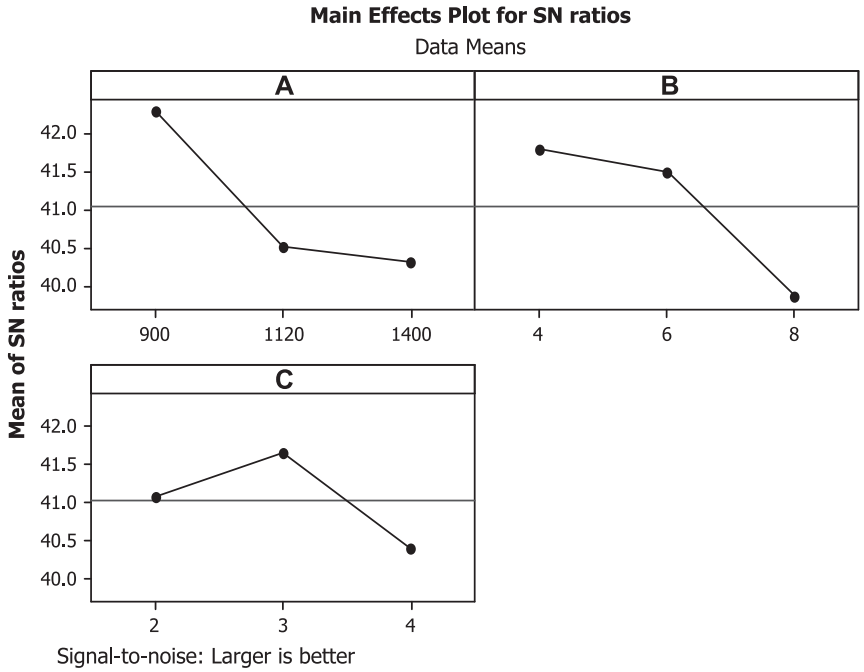

Fig. 11. S/N ratio response graph for YS.

increasing the volume percentage of SiC particles increases the interface area between the SiC particles and aluminum matrix; due to low inter particles space area causes the agglomeration of SiC particle which results in low tensile properties [26]. The volume percentage of SiC particles increase could restrict the grain boundary sliding, dislocations and also the weak interfacial bond between the reinforcement particles and the matrix, finally leading to deterioration of the tensile properties [27,28]. In other words composite has incompatible deformation between the plastically deformed matrix and rigid reinforcement particles causing geometrical dislocations.

It is also observed that the increase in the volume percentage of Al_2O_3 decreases the UTS, YS and %EL. This is due to increase in the interface area between the Al_2O_3 particles and aluminum matrix; due to low inter particles space area causes the agglomeration of Al_2O_3 particles and also increases the presence of micro voids around the Al_2O_3 particles, which results in low tensile properties. Besides, increasing the volume percentage of reinforcement

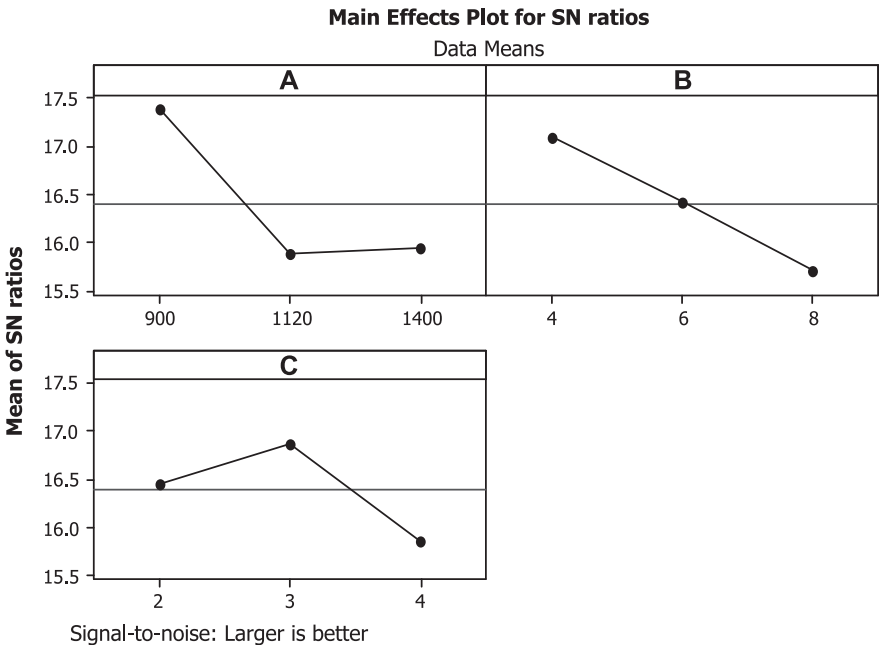

Fig. 12. S/N ratio response graph for %EL.

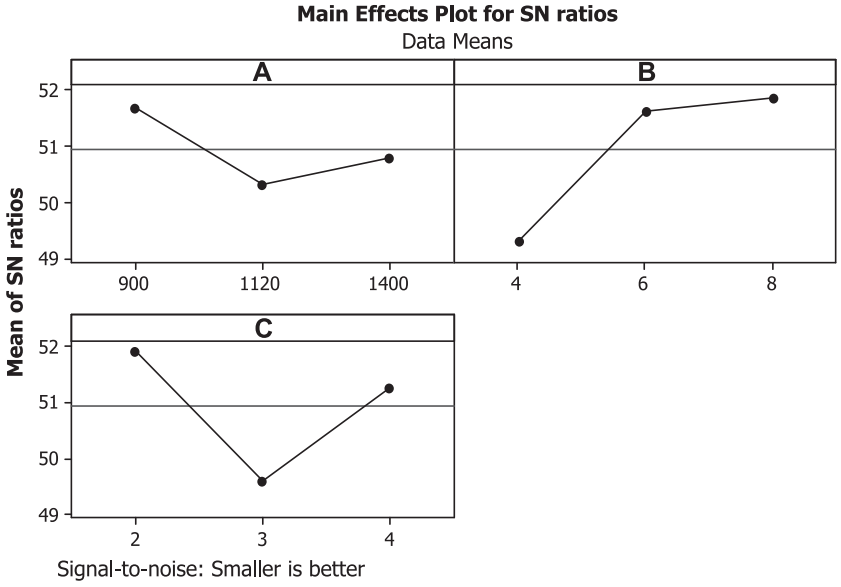

Fig. 13. S/N ratio response graph for wear rate.

particles increases the effective slip distance of dislocations during deformation, which leads to reduce elongation [29].

3.2.6. Effect of process parameters on wear rate

The S/N ratio response graph for wear rate is shown in Fig. 13. It is revealed that the increase in the rotational speed increases the wear rate. It is a well-known fact that increasing the rotation speed, increases the heat generation in the nugget zone which leads to more softening of the matrix due to the over aging [22,24]. The high heat generation causes matrix softening which results in increase the wear rate.

It is observed that the increase in the volume percentage of SiC and Al_2O_3 particles increases the wear rate. At high volume percentage of SiC and Al_2O_3 particles increases the wear rate due to pulled out of hard SiC particles from the composite pin during the wear process, formed on the steel disk which acts as barrier and further converts the adhesive wear to abrasive wear which results in more amount of material worn-out from the composite pin.

The lower wear rate was obtained at the optimum condition of rotational speed of 900 rpm, 8 volume percentage of SiC and 2 volume percentage of Al_2O_3. This is due to the enhanced hardness by the dispersion SiC and Al_2O_3 particles and acted as load-supporting elements [13,30], and the presence of Al_2O_3 which acted as solid lubricant [31]. This is due to the Al_2O_3 particles released on the wear surface during wear process which avoids the direct metal to metal contact and served as a solid lubricant and thereby reduces the coefficient of friction between the composite pin and

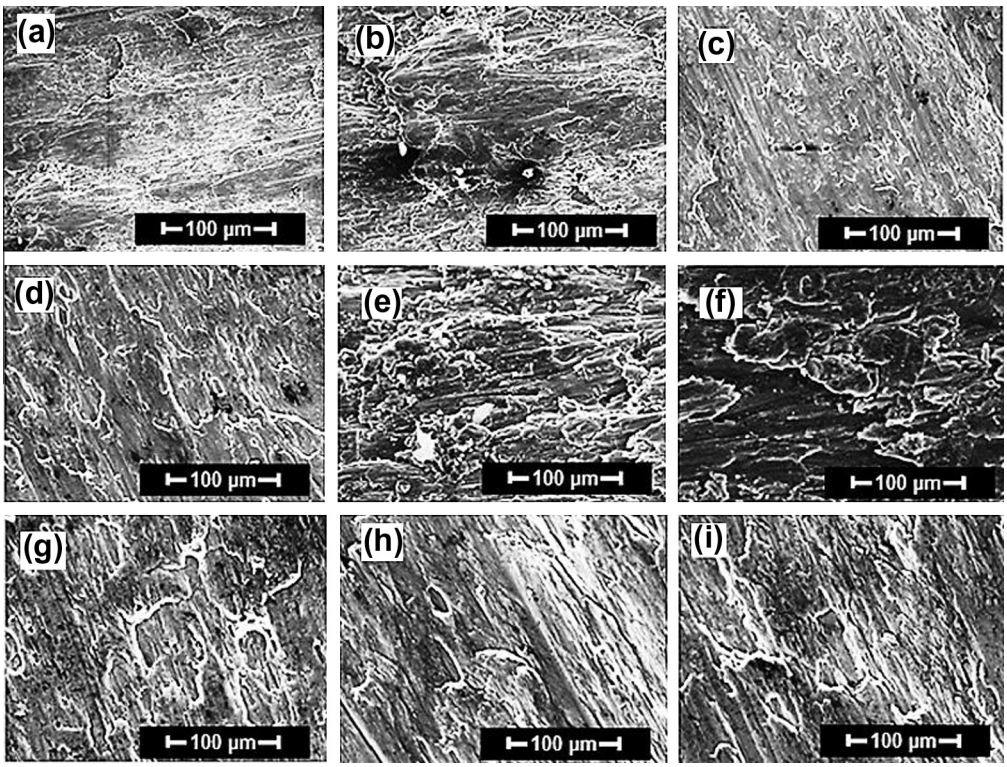

Fig. 14. SEM micrographs of all the worn surface hybrid composites (a) Exp. 1, (b) Exp. 2, (c) Exp. 3, (d) Exp. 4, (e) Exp. 5, (f) Exp. 6, (g) Exp. 7, (h) Exp. 8 and (i) Exp. 9.

the steel disk. Essam et al. [13] and Tjong et al. [31] showed that Al_2O_3 and BN particles were acted as solid lubricant similar to Gr during wear that produces a tinny layer between the deformed surfaces, which decreases the coefficient of friction and enhances the wear resistance.

3.3. Worn morphology

The SEM micrographs of all the worn surface hybrid composites (Exp. 1–9) are shown in Fig. 14. The presence of tribo mechanically mixed layer converts the wear manner into a two body to three body wear and acts as solid lubricant that decreases the wear rate and minimizes the coefficient of friction [13,19,31]. This resulted in decrease of metal removal during wear test. It is observed that the worn debris are more at higher content of SiC and Al_2O_3 particles and less at low content of Al_2O_3 particles. In other words the presence of hard pulled out SiC and Al_2O_3 particles formed on the steel disc which acts as barrier and further it converts the adhesive wear mode into abrasive mode. It is also observed that less cracks and scratches are present at the optimum condition of wear rate (i.e. A1B1C1). It is evident that the presence of enough Al_2O_3 particles acted as a solid lubricant due to formation of a tribo mechanically mixed layer between the two rubbed surfaces (i.e. composite pin and steel disc) which results in lowering the wear rate and similar observations were reported by Essam et al. [13].

4. Conclusions

The influence of reinforcements such as SiC and Al_2O_3 and rotational speed on wear and mechanical properties of aluminum alloy 6061-T6 surface hybrid composites fabricated via FSP were investigated and the following conclusions are obtained.

- The practical benefit of this study is that, the use of obtained optimum condition improves the wear and mechanical properties of surface hybrid composites.
- Microhardness at optimum condition (i.e. A2B1C3) increases due to presence and pining effect of hard SiC and Al_2O_3 particles.
- Wear rate at optimum condition (i.e. A1B1C1) is decreased due to mechanically mixed layer generated between the composite pin and steel disk surfaces which contained fractured SiC and Al_2O_3 in which the presence of SiC particles serves as load bearing elements and Al_2O_3 particles acted as solid lubricant and also load bearing elements.
- Tensile properties at optimum condition (i.e. A1B3C2) are less as compared to the base material due to presence of reinforcement particles which make the matrix brittle.
- Regression models were developed to predict the quality characteristics (microhardness, UTS, YS, %EL and wear rate) within the selected range of process parameters (SiC, Al_2O_3 and rotational speed). The results are validated through ANOVA.

Acknowledgements

The authors would like to thank the authorities of National Institute of Technology-Warangal, Defence Metallurgical Research Laboratory-Hyderabad, Indian Institute of Chemical Technology-Hyderabad, Defence Institute of Advanced Technology-Pune and Research Centre Imarat–Hyderabad for providing the facilities to carry out this work.

References

[1] Bakes H, Benjamin D, Kirkpatrick CW. Metals handbook, vol. 2. ASM, Metals Park: OH; 1979; p. 3–23.
[2] Ravi N, Sastikumar D, Subramanian N, Nath AK, Masilamani V. Microhardness and microstructure studies on laser surface alloyed aluminium alloy with Ni–Cr. Mater Manuf Process 2000;15:395–404.
[3] Clyne TW, Withers PJ. An introduction to metal matrix composites. Cambridge: Cambridge University Press; 1993.
[4] Rabinowicz E. Friction and wear of materials. New York: JohnWiley and Sons; 1965.

[5] Budinski KG. Surface engineering for wear resistance. New Jersey: Prentice-Hall; 1988.
[6] Gupta M, Mohamed FA, Lavernia EJ. Solidification behaviour of Al–Li–SiCp MMCs processed using variable co-deposition of multi-phase materials. Mater Manuf Process 1990;5(2):165–96.
[7] Mabhali LAB, Pityana SL, Sacks N. Laser surface alloying of aluminum (AA1200) with Ni and SiC powders. Mater Manuf Process 2010; 25(12):1397–403.
[8] Mishra RS, Ma ZY, Charit I. Friction stir processing: a novel technique for fabrication of surface composites. Mater Sci Eng A 2003;341:307–10.
[9] Ma ZY. Friction stir processing technology: a review. Metall Mater Trans A 2008;39:642–58.
[10] Asadi P, Besharati Givi MK, Faraji G. Producing ultrafine-grained AZ91 from As-Cast AZ91 by FSP. Mater Manuf Process 2010;25(11):1219–26.
[11] Dehghani K, Mazinani M. Forming nanocrystalline surface layers in copper using friction stir processing. Mater Manuf Process 2011;26(07):922–5.
[12] Devaraju A, Kumar A. Dry sliding wear and static immersion corrosion resistance of aluminum alloy 6061–T6/SiCp metal matrix composite prepared via friction stir processing. Int J Adv Res Mech Eng 2011;1(2):62–8.
[13] Essam RI, Makoto T, Tishiya S, Kenji I. Wear characteristics of surface-hybrid-MMCs layer fabricated on aluminum plate by friction stir processing. Wear 2010;268:1111–21.
[14] Ross PJ. Taguchi techniques for quality engineering. New York: Mc Graw-Hill; 1998. p. 24–98.
[15] Montgomery DC. Design and analysis of experiments. Wiley: New York; 1997. p. 395–476.
[16] Phadke Madhav S. Quality engineering using robust design. New Jersey: Prentice Hall, Englewood Cliffs; 1989. p. 41–229.
[17] Mallaiah G, Kumar A, Ravinder Reddy P, Madhusudan Reddy G. Influence of grain refine elements on mechanical properties of AISI 430 ferritic stainless steel weldments-Taguchi approach. Mater Des 2012;36:443–50.
[18] Gurcan AB. Wear behaviour of AA6061 aliminum alloy and its composites. Wear 1995;188:185–91.
[19] Hayrettin A. Wear behaviour of Al/(Al_2O_{3p}/SiC_p) hybrid composites. Tribol Int 2006;39:213–20.
[20] Kocer T. Investigation of wear behaviour of Al_2O_3 and SiC reinforced Al–Mg metal matrix composites produced by pressure infiltration technique. MS thesis. Istanbul Technical University; 2002 [in Turkish].
[21] Basavarajappa S. Influence of sliding speed on the dry sliding wear behaviour and the subsurface deformation on hybrid metal matrix composite. Wear 2007;262:1007–12.
[22] Olga VF. Microstrucural issues in a friction stir welded aluminium alloys. Scr Mater 1998;38(5):703–8.
[23] Gupta M, Lai MO, Soo CY. Effect of type of processing on the microstructural features and mechanical properties of Al–Cu/SiC metal matrix composites. Mater Sci Eng A 1996;210:114–22.
[24] Shafiei ZA, Rashani Bozorg SF, Zarei H. Microstructure and mechanical properties of Al/Al_2O_3 surface nano-composite layer produced by friction stir processing. Mater Sci Eng A 2009;500:84–91.
[25] Morisada Y, Fujii H, Nagaoka T, Fucksumi M. Effect of friction stir processing with SiC particles on microstructure and hardness of AZ31. Mater Sci Eng A 2006;433:50–4.
[26] Muratoglu M, Yilmaz O, Aksoy M. Investigation on diffusion bonding characteristics of aluminium metal matrix composites (Al/SiC_p) with pure aluminium for different heat treatments. J Mater Process Technol 2006;178:211–7.
[27] Barmouz M, Kazem Besharati G, Javad S. On the role of processing parameters in producing Cu/SiC metal matrix composites via friction stir processing: Investigating microstructure, microhardness, wear and tensile behaviour. Mater Charact 2011;62:108–17.
[28] Barmouz M, Asadi P, Besharati Givi MK, Taherishargh M. Investigation of mechanical properties of Cu/SiC composite fabricated by FSP: Effect of SiC particles' size and volume fraction. Mater. Sci. Eng. A 2011;528:1740–9.
[29] Hai Su, Wenli G, Zhaohui F, Zheng L. Processing, microstructure and tensile properties of nano-sized Al_2O_3 particles reinforced aluminium matrix composites. Mater Des 2012;36:590–6.
[30] Kumar S, Balasubramanian V. Developing mathematical model to calculate wear rate of AA7075/SiC_p powder metallurgy composite. Wear 2008;264:1026–34.
[31] Tjong SC, Lau KC, Wu SQ. Wear of Al-based hybrid composites containing BN and SiC particulates. Metall Mater Trans A 1999;30A:2551–5.